

# Hybrid model of proton structure functions

S.A. Kulagin<sup>1</sup>, V.V. Barinov<sup>1,2</sup>

*<sup>2</sup>Lomonosov Moscow State U.*

*<sup>1</sup>Moscow, INR*

*Phys.Rev.C 105 (2022) 045204*

Dubna

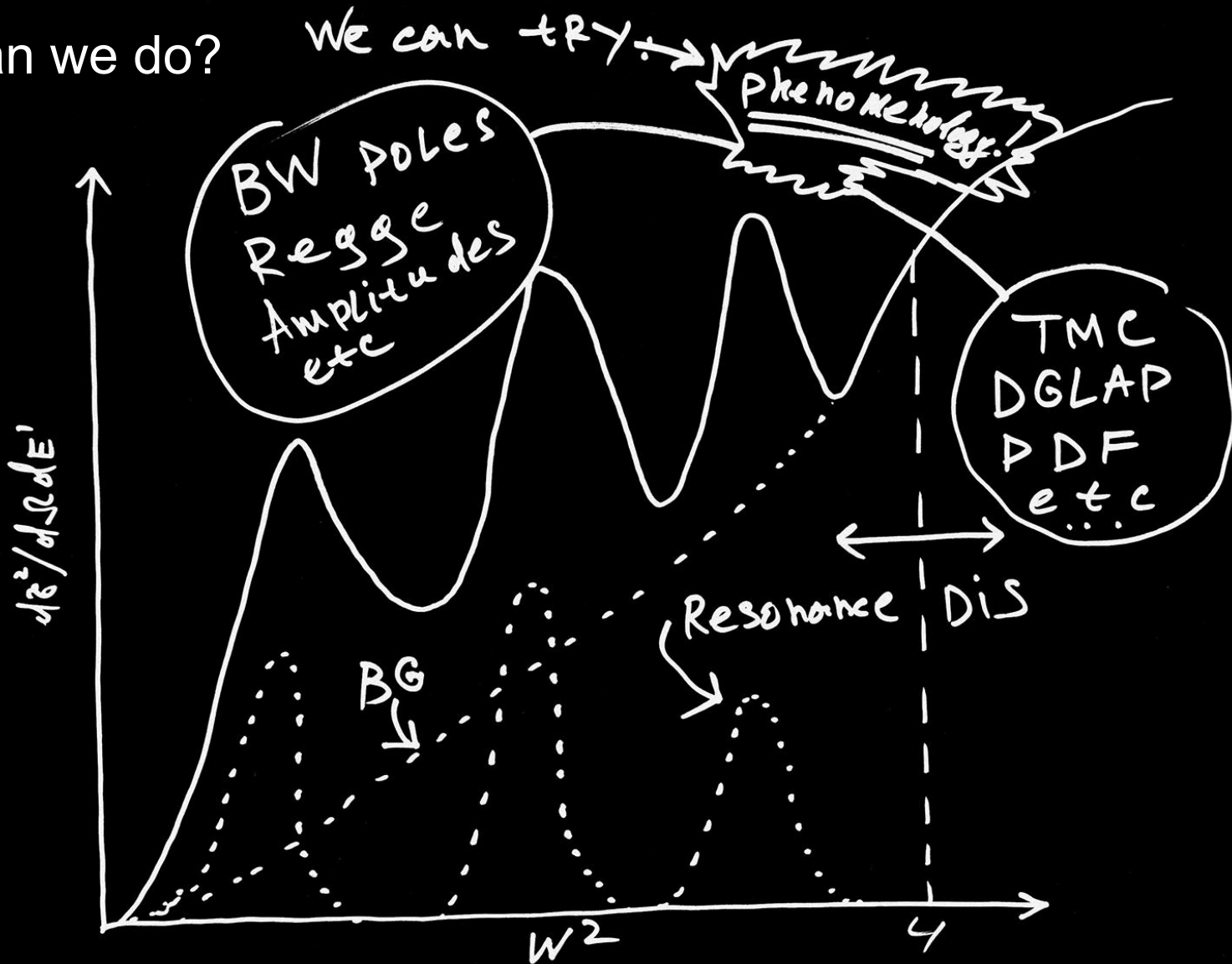
2022

# Motivation

- As the values of  $Q$  and  $W$  decrease various subleading effects, such as higher-order perturbative QCD corrections in the strong coupling constant, higher-twist power corrections and/or target mass corrections become increasingly important.
- In a strong coupling regime at a low scale  $Q < 1$  GeV available methods of perturbative QCD, the twist expansion, and the methods based on the renormalization group equations are not applicable and the validity of the partonic picture becomes controversial.
- There are many experiments in resonance and DIS regions. Nevertheless, self consistent data analysis and good quality data description are difficult to do...

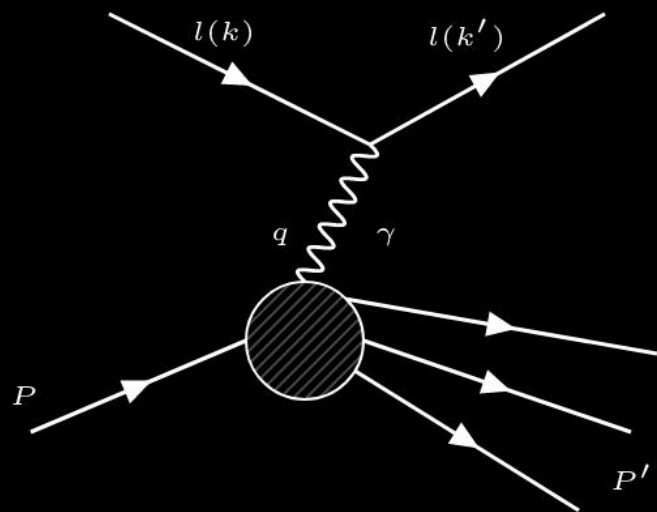
What can we do?

We can try →



# Introduction

$$e + p \rightarrow e + X$$



$$W_{\mu\nu}(p, q) = \frac{1}{8\pi} \sum_{\lambda, n} (2\pi)^4 \delta(p + q - p_n) \langle P, \lambda | J_\mu^{\text{em}}(0) | n \rangle \langle n | J_\nu^{\text{em}}(0) | P, \lambda \rangle$$

$$W_{\mu\nu}(p, q) = \left( \frac{q_\mu q_\nu}{q^2} - g_{\mu\nu} \right) F_1 + \frac{F_2}{p \cdot q} \left( p_\mu - q_\mu \frac{p \cdot q}{q^2} \right) \left( p_\nu - q_\nu \frac{p \cdot q}{q^2} \right)$$

$$\frac{d^2\sigma}{dx dQ^2} = \frac{4\pi\alpha^2}{xQ^4} \left[ xy^2 \left( 1 - \frac{2m_l^2}{Q^2} \right) F_1 + \left( 1 - y - \frac{M^2 x^2 y^2}{Q^2} \right) F_2 \right]$$

$$\frac{d^2\sigma}{d\Omega dE'} = \frac{x E'}{\pi y} \frac{d^2\sigma}{dx dQ^2}$$

# Introduction / Resonance and DIS Region

$$\frac{d^2\sigma}{dx dQ^2} = \frac{4\pi\alpha^2}{xQ^4} \left[ xy^2 \left( 1 - \frac{2m_l^2}{Q^2} \right) F_1 + \left( 1 - y - \frac{M^2 x^2 y^2}{Q^2} \right) F_2 \right]$$

**Resonance Region:**

$$F_T^{\text{Res}} = \frac{xM}{2\pi\alpha} \sum_R \delta(W^2 - M_R^2)(M_R^2 - M^2) (|A_{1/2}^R(Q^2)|^2 + |A_{3/2}^R(Q^2)|^2),$$

$$F_L^{\text{Res}} = \frac{xM}{\pi\alpha} \sum_R \delta(W^2 - M_R^2)(M_R^2 - M^2) \frac{Q^2}{|\mathbf{q}|_{\text{CM}}^2} |S_{1/2}^R(Q^2)|^2,$$

$$\delta(W^2 - M_R^2) \rightarrow \frac{1}{\pi} \frac{M_R \Gamma_R}{(W^2 - M_R^2)^2 + M_R^2 \Gamma_R^2}$$

**DIS Region:**

$$F_i^{\text{DIS}}(x, Q^2) = F_i^{\text{TMC}}(x, Q^2) + H_i(x)/Q^2 + \mathcal{O}(Q^{-4}) \longrightarrow \text{Alekhin Global Fit}$$

$$F_T = x \sum_{m=\pm 1} \varepsilon_\mu^{(m)*} W_{\mu\nu} \varepsilon_\nu^{(m)} = 2x F_1$$

$$F_L = 2x \varepsilon_\mu^{(0)} W_{\mu\nu} \varepsilon_\nu^{(0)} = \gamma^2 F_2 - F_T$$

$$\gamma^2 = 1 + 4x^2 M^2 / Q^2$$

# Framework

$$F_i = F_i^{\text{Res}} + F_i^{\text{BG}}$$

## Resonance Part

$$|A(Q^2)|^2 = |A_{1/2}(Q^2)|^2 + |A_{3/2}(Q^2)|^2$$

Note that the unpolarized scattering is not sensitive to individual amplitudes  $A_{1/2}$  and  $A_{3/2}$  and only their quadrature sum is relevant. For this reason, for each of the resonance state we use the average amplitude  $A(Q^2)$  defined as

$$A(Q^2) = (a_1 + a_2 Q^2) / (1 + a_3 Q^2)^{a_4}$$
$$S_{1/2}(Q^2) = (c_1 + c_2 Q^2) \exp(-c_3 Q^2)$$

## Background Part

$$F_i^{\text{BG}} = B_i(W^2) \begin{cases} F_i^{\text{DIS}}(W^2, Q^2) & \text{if } Q^2 \geq Q_0^2, \\ F_i^{\text{Ext}}(W^2, Q^2) & \text{if } Q^2 < Q_0^2, \end{cases}$$

The factors  $B_T$  and  $B_L$  are responsible for extrapolation to the low- $W$  region and in this study we assume them to be the functions of  $W$  only.

The  $B_{T,L}$  functions are positively defined and required to vanish at the pion production threshold  $W \rightarrow W_{\text{th}} = M + m_\pi$ .

$$B = 1 - \exp(-b_1(W^2 - W_{\text{th}}^2)^{b_2})$$

# Framework / Extrapolation Functions

$$F_i = F_i^{\text{Res}} + F_i^{\text{BG}}$$

$$F_i^{\text{BG}} = B_i(W^2) \begin{cases} F_i^{\text{DIS}}(W^2, Q^2) & \text{if } Q^2 \geq Q_0^2, \\ F_i^{\text{Ext}}(W^2, Q^2) & \text{if } Q^2 < Q_0^2, \end{cases}$$

## Background Extrapolation Functions

$$F_T^{\text{Ext}}(W^2, t) = f_0 t + f_1 t^m + f_2 t^n$$

$$F_L^{\text{Ext}}(W^2, t) = f'_1 t^{m'} + f'_2 t^{n'}$$

The functions  $f_1$  and  $f_2$  are determined by requiring the smoothness of the extrapolation function at  $t = t_0 = Q_0^2$ ; i.e., we require the continuity of the function and its first derivative at the DIS matching point.

$$F_T^{\text{Ext}} = f_0 t + \left(\frac{t}{t_0}\right)^m \left[ F_T^{\text{DIS}} - f_0 t_0 + (m F_T^{\text{DIS}} - t_0 \partial_t F_T^{\text{DIS}} - (m-1) f_0 t_0) \ln \frac{t_0}{t} \right]$$

$$F_L^{\text{Ext}} = \left(\frac{t}{t_0}\right)^{m'} \left[ F_L^{\text{DIS}} + (m' F_L^{\text{DIS}} - t_0 \partial_t F_L^{\text{DIS}}) \ln \frac{t_0}{t} \right]$$

# Data and Fit

$$\chi^2 = \sum_i (v_i^{\text{exp}} - v_i^{\text{mod}})^2 / \sigma_i^2$$

Hydrogen **electroproduction cross-section** data sets used in our analysis. Listed are the experiments with corresponding number of data points (NDP) and kinematics coverage.

The values of  $Q^2$  and  $W^2$  are in  $\text{GeV}^2$  units. The cut  $W^2 > 1.16 \text{ GeV}^2$  was applied.

The last two columns are the values of  $\chi^2$  normalized per NDP computed, respectively, in our model and in the model of Ref. [5], for comparison.

Data set <sup>a</sup>	NDP	$Q_{\min}^2$	$Q_{\max}^2$	$W_{\min}^2$	$W_{\max}^2$	$\chi^2$	$\chi_{\text{CB}}^2$
SLAC-E49a (DIS) [28]	117	0.586	8.067	3.130	27.19	0.55	N/A
SLAC-E49b (DIS) [28]	208	0.663	20.08	3.010	27.51	1.32	N/A
SLAC-E61 (DIS) [28]	32	0.581	1.738	3.210	16.00	0.44	N/A
SLAC-E87 (DIS) [28]	109	3.959	20.41	3.280	17.18	0.57	N/A
SLAC-E89a (DIS) [28]	77	3.645	30.31	3.300	20.43	0.60	N/A
SLAC-E89b (DIS) [28]	118	0.887	19.18	3.100	27.75	0.70	N/A
SLAC-E004 (DIS) [29]	198	0.249	20.07	3.561	26.84	0.44	N/A
SLAC-E49a6 (RES) [29]	460	0.146	3.708	1.177	3.992	0.72	1.16
SLAC-E49a10 (RES) [29]	541	0.445	8.593	1.171	4.000	0.84	1.04
SLAC-E49b (RES) [29]	366	1.018	16.74	1.153	3.992	0.81	1.15
SLAC-E61 (RES) [29]	1075	0.061	1.839	1.160	4.000	1.20	1.76
SLAC-E87 (RES) [29]	22	1.821	20.54	3.183	3.988	0.25	N/A
SLAC-E89a <sup>b</sup> (RES) [29]	90	7.124	32.39	1.156	4.000	0.14	N/A
SLAC-E89b <sup>c</sup> (RES) [29]	492	0.395	20.66	1.197	3.984	1.12	N/A
SLAC-E133 (RES) [29]	178	2.287	9.914	1.153	3.037	3.19	5.04
SLAC-E140 (RES) [29]	87	0.717	20.41	3.010	3.950	1.46	N/A
SLAC-E140X (RES) [29]	153	1.118	8.871	1.200	3.720	2.88	3.27
SLAC-NE11 (RES) [30]	113	1.606	6.855	1.164	1.788	2.27	5.78
SLAC-Onen1half (RES) [29]	745	0.011	0.263	1.153	4.000	6.18	7.00
Jlab-CLAS E1 <sup>d</sup> (RES) [31–34]	509	0.225	0.925	1.162	2.544	1.15	19.5
Jlab-CLAS E2 (RES) [31–34]	1443	0.475	2.175	1.162	3.987	1.44	11.3
Jlab-CLAS E3 (RES) [31–34]	2484	1.325	4.175	1.162	5.537	1.04	2.73
Jlab-CLAS E4 (RES) [31–34]	2637	1.325	4.425	1.164	5.643	0.95	1.93
Jlab-CLAS E5 (RES) [31–34]	2681	1.375	4.725	1.162	5.971	0.96	1.51
JLab-E94-110 (RES) [29]	1273	0.181	5.168	1.225	3.850	3.15	1.33
JLab-E00-116 (RES) [35]	261	3.585	7.384	1.243	5.131	1.48	1.58
JLab-E00-002 (RES) [29, 36]	1477	0.055	2.079	1.163	7.932	1.22	0.88



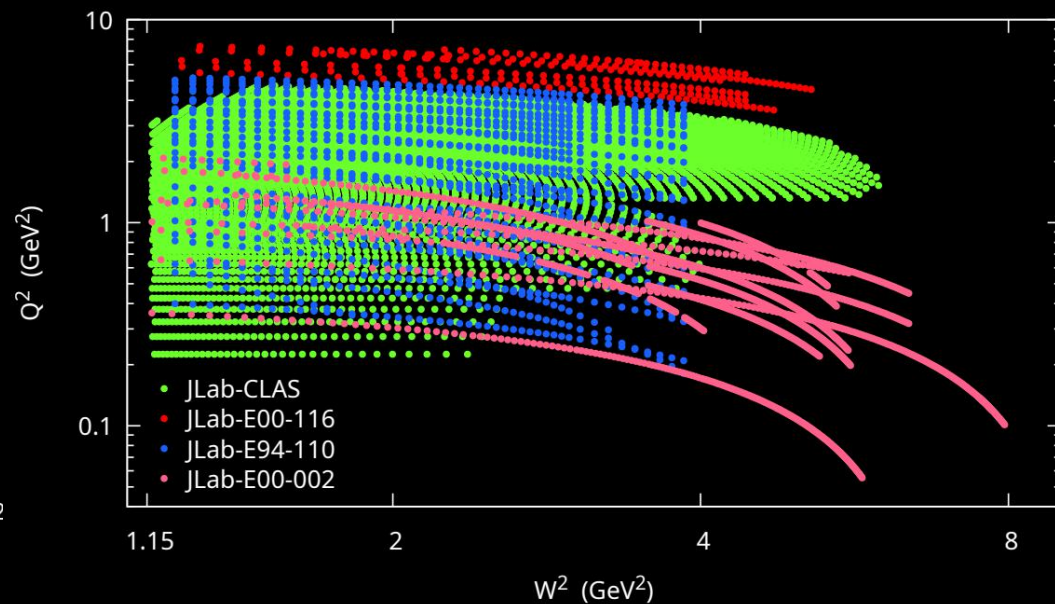
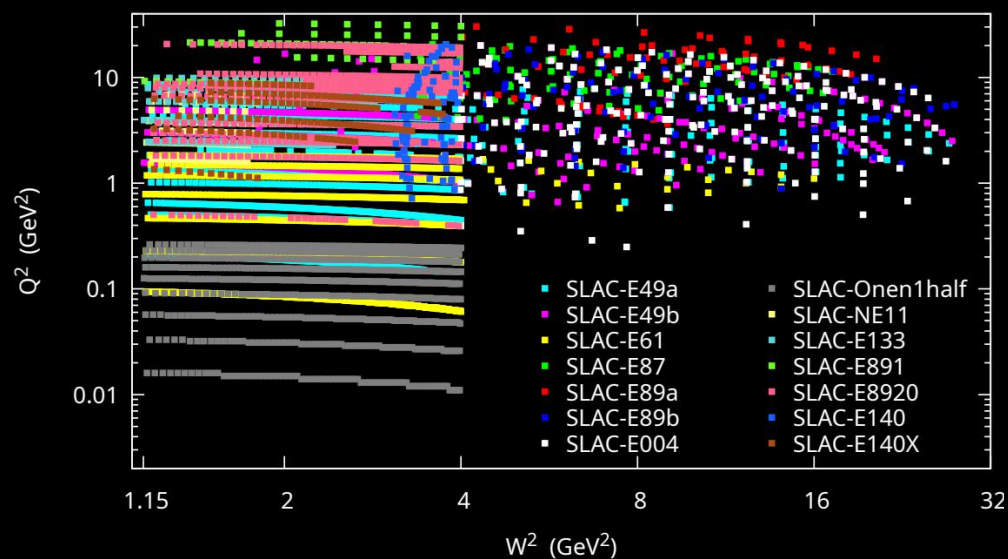
# Data and Fit

Hydrogen **photoproduction cross section** data sets used in our analysis. Listed are the experiments with corresponding number of data points (NDP) and kinematics coverage. The values of  $W^2$  are in  $\text{GeV}^2$  units.

The last two columns are the values of  $\chi^2$  normalized per NDP computed in our model and in the model of Ref. [5], respectively.

Data set	NDP	$W_{\min}^2$	$W_{\max}^2$	$\chi^2$	$\chi_{\text{CB}}^2$
Armstrong [37]	159	1.378	8.790	2.39	1.34
Maccormick [38]	57	1.263	2.361	2.15	7.12
Meyer [39]	18	3.038	12.61	0.69	0.54
Hilpert [40]	6	2.121	9.212	3.09	1.66
Dieterle [41]	5	2.382	11.67	1.70	N/A
Ballam [42]	3	6.135	14.95	0.79	N/A
Bingham [43]	1	18.33	18.33	0.26	N/A
Caldwell [44]	9	8.518	31.62	1.10	N/A
Caldwell [45]	30	35.22	343.7	0.64	N/A
Michalowski [46]	6	4.633	18.73	1.08	N/A
Alexander [47]	1	14.95	14.95	0.003	N/A
Aid [48]	2	39999	43681	0.27	N/A
Vereshkov [49]	4	2065	17822	0.24	N/A
GRAAL [50]	62	1.950	3.564	9.92	6.50

# Kinematic Region Example



# Data and Fit

Standard Chi squared approach

$$\chi^2 = \sum_i (v_i^{\text{exp}} - v_i^{\text{mod}})^2 / \sigma_i^2$$

*Statistics<sup>2</sup> + Systematics<sup>2</sup> + Normalization<sup>2</sup>*

MINUIT + 68 Initial Parameters

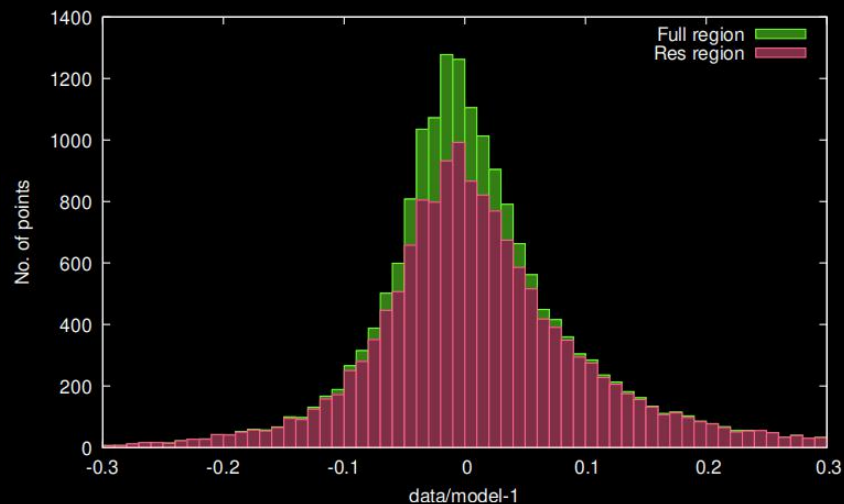
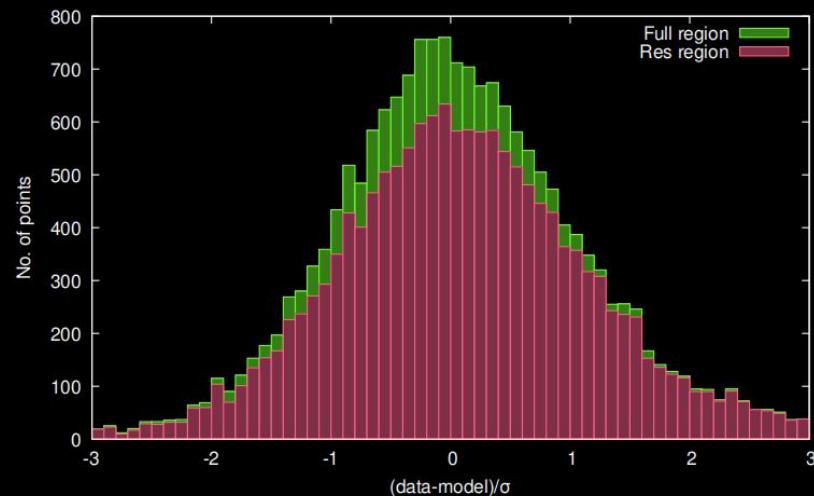
## Problems

Iterative Procedure

Local Minimum Selection

*It's looks like fine tuning :)*

**But we have the stable results!**



# Best Fit Parameters

TABLE I. The best fit values for the mass  $M_R$ , the intrinsic width  $\Gamma_R$ , the angular momentum  $L$ , the damping parameter  $X_R$ , and the decay branching fractions  $\beta$  for each of the resonant state. The dimensional parameters are in GeV units. The estimate of the fit parameter uncertainty is given in parentheses in percent units.

	$M_R$	$\Gamma_R$	$L$	$X_R$	$\beta_{1\pi}$	$\beta_{2\pi}$	$\beta_\eta$
$\Delta(1232)$	1.2270(0.02)	0.1128(0.48)	1	0.0554(1.07)	1.00	0.00	0.00
$N(1440)$	1.4487(0.34)	0.4022(3.34)	1	0.1125(3.85)	0.65	0.35	0.00
$R_1$	1.5123(0.02)	0.0945(1.83)	2	0.4959(4.81)	0.75	0.25	0.00
$R_2$	1.5764(0.16)	0.5005(1.76)	0	0.3097(2.12)	0.15	0.85	0.00
$R_3$	1.7002(0.03)	0.1177(1.66)	2	0.2583(10.8)	0.15	0.60	0.25

TABLE IV. The best fit parameters describing the resonant contributions to the transverse helicity amplitude by Eq. (32). The estimate of fractional parameter uncertainty is given in parentheses in percent units.

	$a_1$ (GeV $^{-1/2}$ )	$a_2$ (GeV $^{-5/2}$ )	$a_3$ (GeV $^{-2}$ )	$a_4$
$\Delta(1232)$	0.31115(0.31)	2.02940(0.57)	1.67130(1.06)	2.7600(0.41)
$N(1440)$	0.08955(4.61)	0.18087(1.16)	0.23431(0.87)	4.1173(0.35)
$R_1$	0.10677(2.08)	0.24897(1.62)	0.55621(0.66)	3.0798(0.38)
$R_2$	0.38953(0.60)	-0.17962(1.88)	0.37638(3.09)	2.9622(1.70)
$R_3$	0.06708(5.72)	0.09733(6.26)	0.27891(4.74)	3.5372(1.42)

TABLE V. The best fit parameters describing the resonant contributions to the longitudinal helicity amplitude by Eq. (33). The estimate of fractional parameter uncertainty is given in parentheses in percent.

	$c_1$ (GeV $^{-1/2}$ )	$c_2$ (GeV $^{-5/2}$ )	$c_3$ (GeV $^{-2}$ )
$\Delta(1232)$	0.05029(6.72)	0	0.42522(6.40)
$N(1440)$	0	0.23847(2.62)	1.4982(2.03)
$R_1$	0.09198(4.33)	-0.10652(5.81)	1.0758(3.48)
$R_2$	0	0	0
$R_3$	0.12027(1.68)	0	0.89367(2.72)

TABLE VI. The best fit parameters describing the background function by Eq. (42). The estimate of fractional parameter uncertainty is given in parentheses in percent.

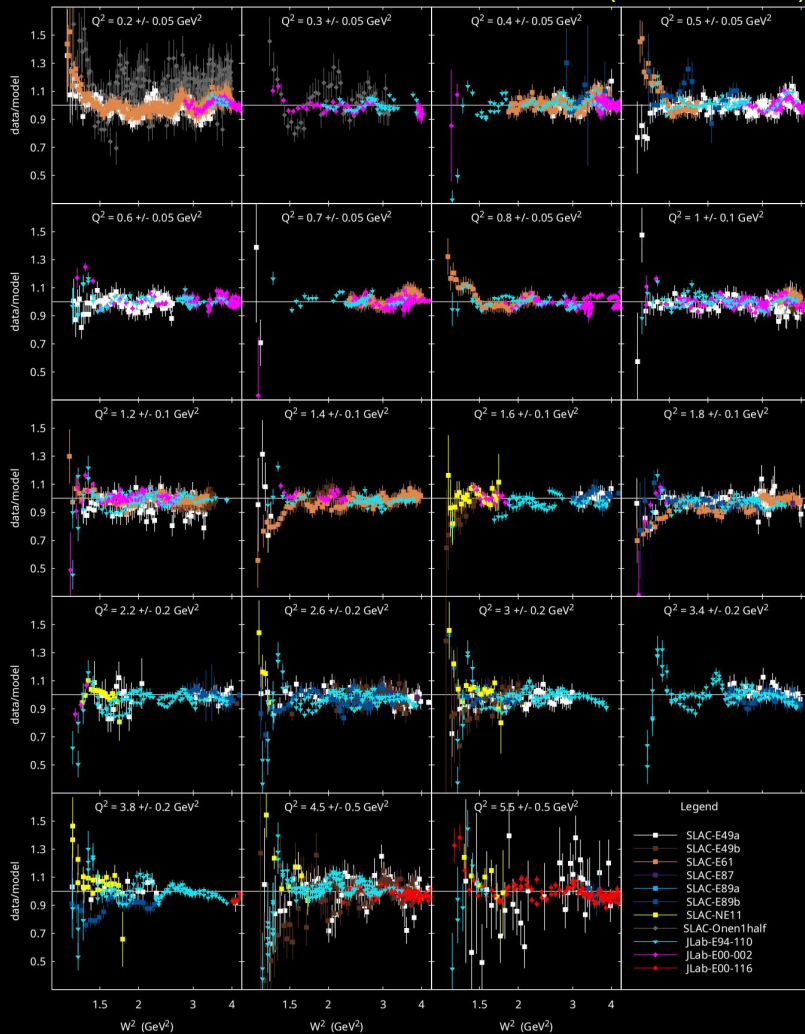
	$b_1$ (GeV $^{-2b_2}$ )	$b_2$	$m_{T,L}$
$B_T$	0.14453(4.19)	3.1297(1.76)	1.6302(0.19)
$B_L$	3.4742(2.44)	0.54193(1.26)	1.1



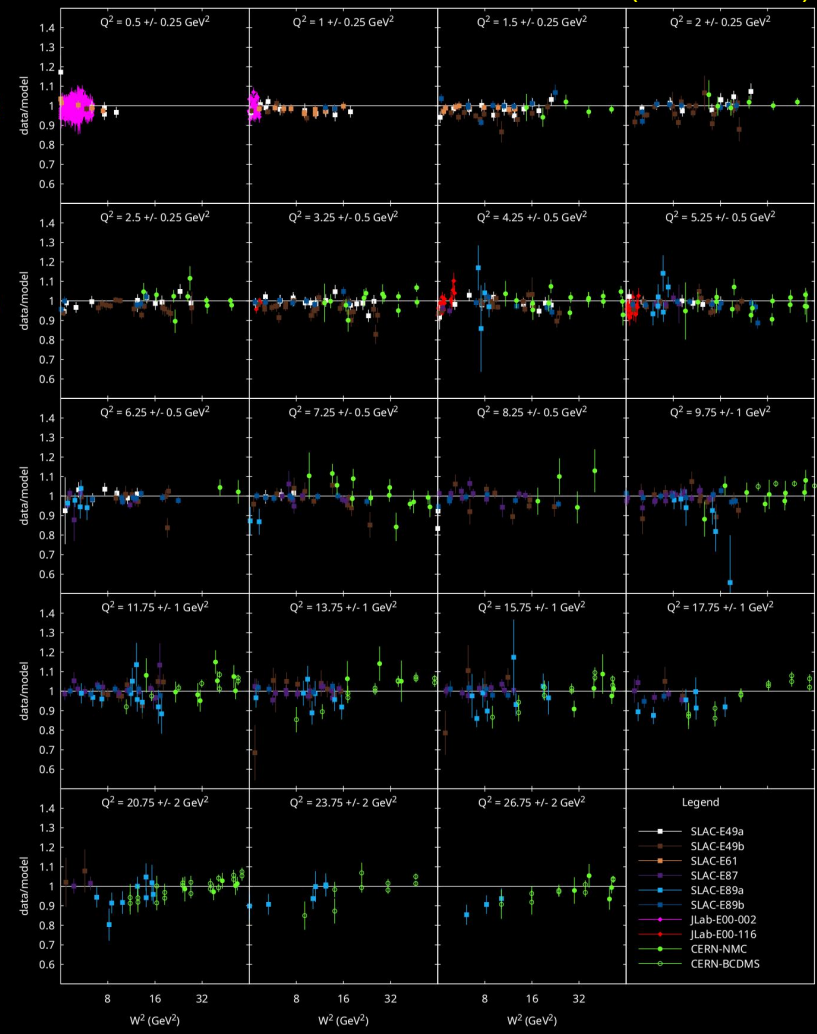
# Cross Section Results (Training Data)

Data set <sup>a</sup>	NDP	$\chi^2$
SLAC-E49a (DIS) [29]	117	0.55
SLAC-E49b (DIS) [29]	208	1.32
SLAC-E61 (DIS) [29]	32	0.44
SLAC-E87 (DIS) [29]	109	0.57
SLAC-E89a (DIS) [29]	77	0.60
SLAC-E89b (DIS) [29]	118	0.70
SLAC-E004 (DIS) [30]	198	0.44
SLAC-E49a6 (RES) [30]	460	0.72
SLAC-E49a10 (RES) [30]	541	0.84
SLAC-E49b (RES) [30]	366	0.81
SLAC-E61 (RES) [30]	1075	1.20
SLAC-E87 (RES) [30]	22	0.25
SLAC-E89a <sup>b</sup> (RES) [30]	90	0.14
SLAC-E89b <sup>c</sup> (RES) [30]	492	1.12
SLAC-E133 (RES) [30]	178	3.19
SLAC-E140 (RES) [30]	87	1.46
SLAC-E140X (RES) [30]	153	2.88
SLAC-NE11 (RES) [31]	113	2.27
SLAC-Onen1half (RES) [30]	745	6.18
Jlab-CLAS E1 <sup>d</sup> (RES) [32-35]	509	1.15
Jlab-CLAS E2 (RES) [32-35]	1443	1.44
Jlab-CLAS E3 (RES) [32-35]	2484	1.04
Jlab-CLAS E4 (RES) [32-35]	2637	0.95
Jlab-CLAS E5 (RES) [32-35]	2681	0.96
JLab-E94-110 (RES) [30]	1273	3.15
JLab-E00-116 (RES) [36]	261	1.48
JLab-E00-002 (RES) [30, 37]	1477	1.22

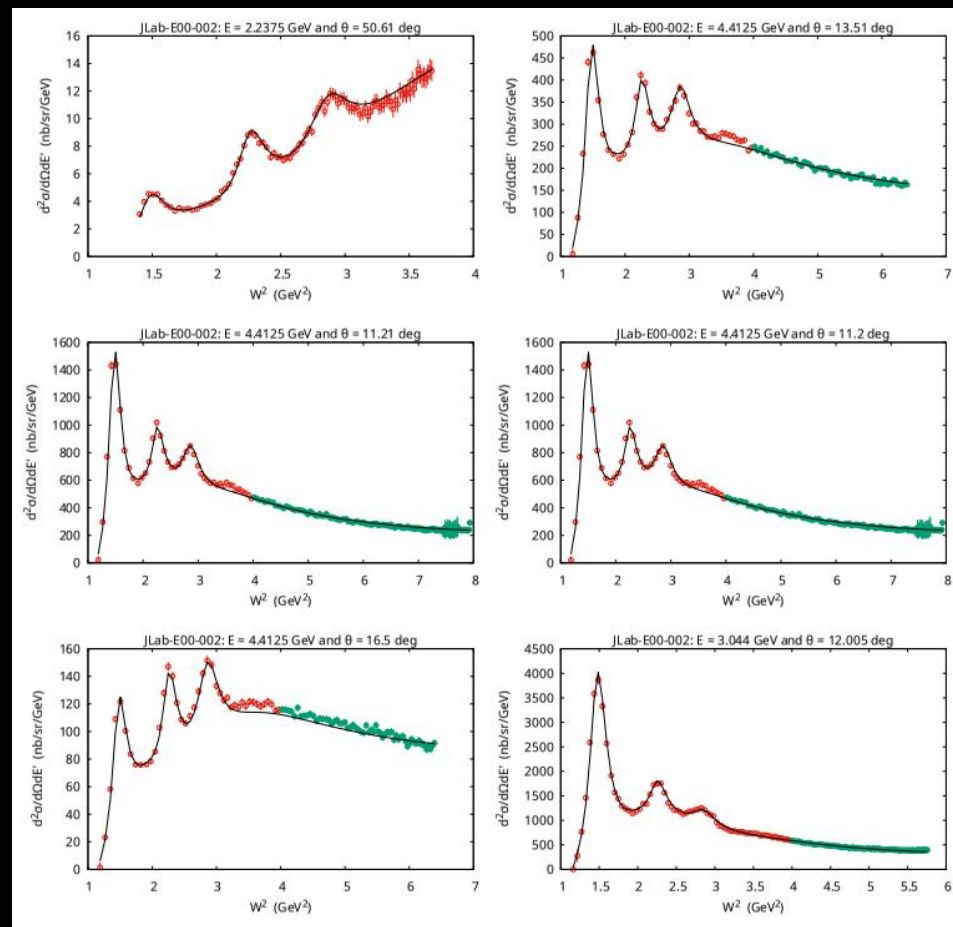
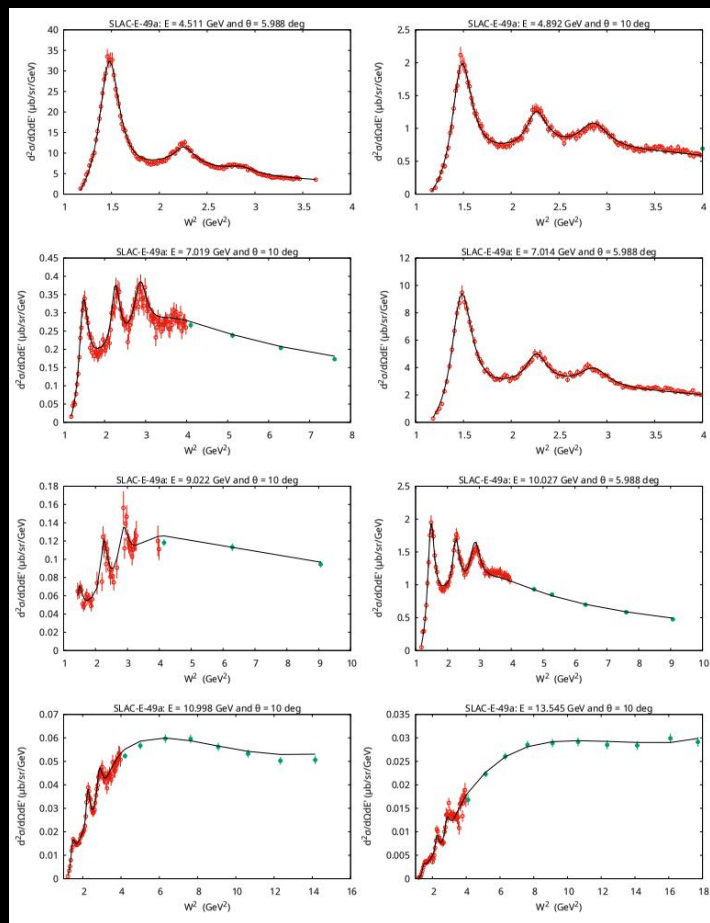
Resonance ( $W^2 < 4 \text{ GeV}^2$ )



DIS ( $W^2 > 4 \text{ GeV}^2$ )



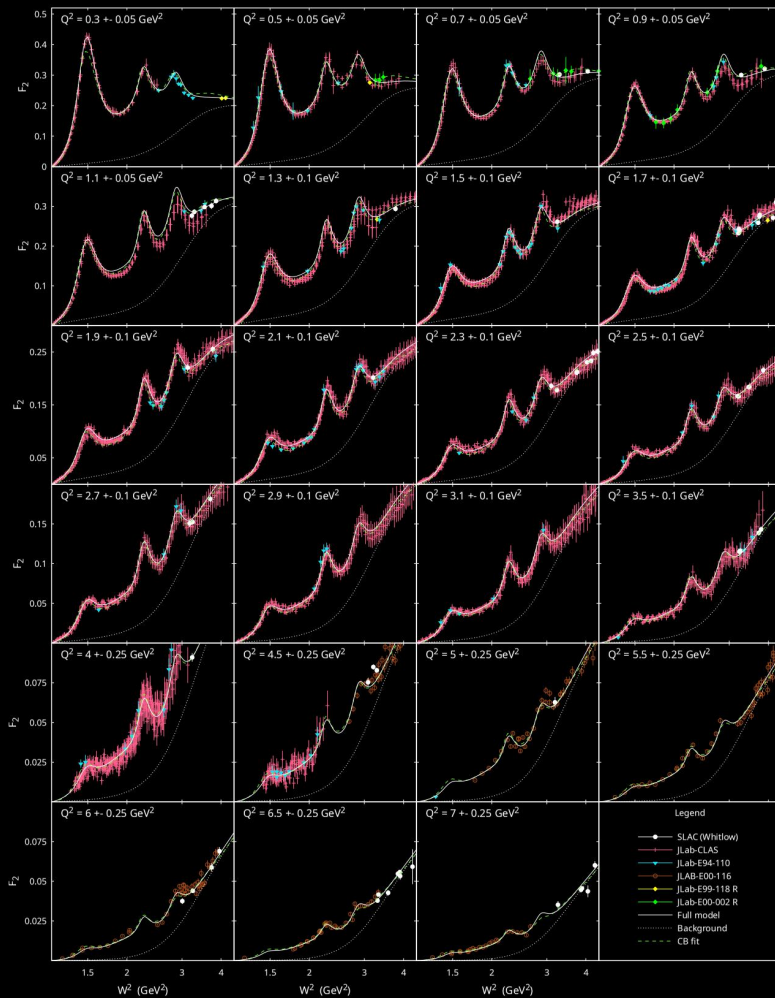
# Cross Section Data Visualization



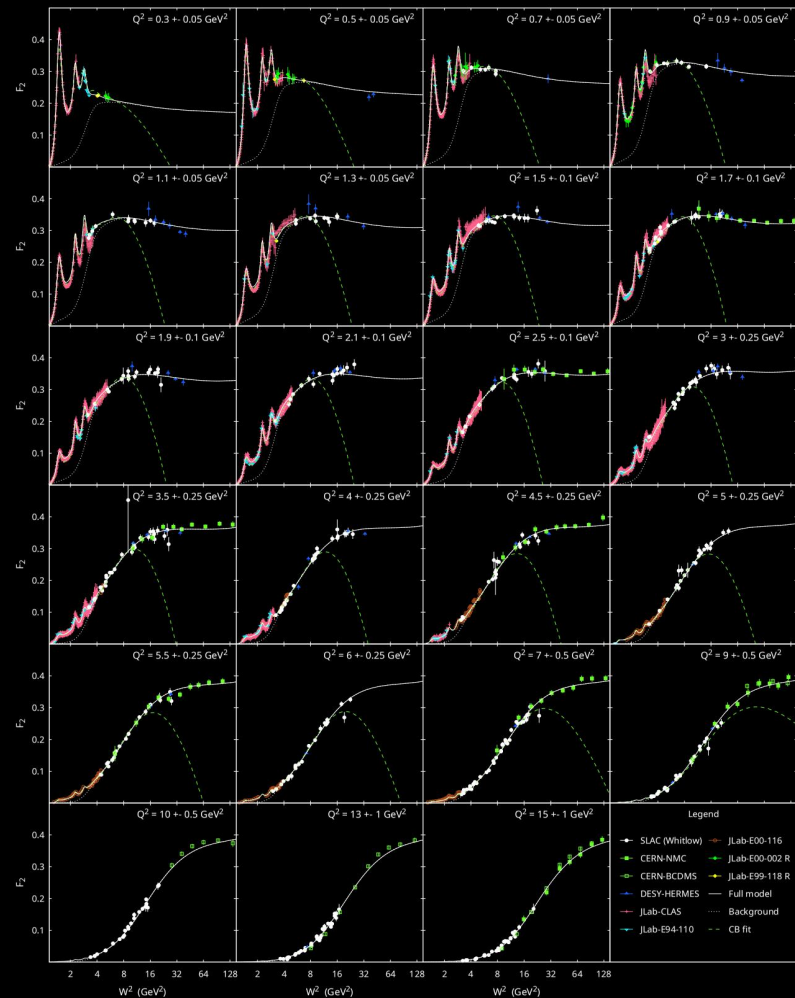
# F2 Results (Test Data)

$F_2$ data set	NDP	$\chi^2$
SLAC-E49a [29] (DIS)	117	0.50
SLAC-E49b [29] (DIS)	208	0.72
SLAC-E61 [29] (DIS)	32	0.34
SLAC-E87 [29] (DIS)	109	0.59
SLAC-E89a [29] (DIS)	77	1.01
SLAC-E89b [29] (DIS)	118	0.52
JLab-CLAS [33] (RES)	4191	1.17
JLab-E94-110 [68] (RES)	170	1.90
JLab-E00-116 [69] (RES)	261	1.42
JLab-E00-002 [37] (RES)	54	0.24
CERN-NMC [62] (DIS)	157	1.74
CERN-BCDMS [63] (DIS)	177	2.31
DESY-HERMES [67] (DIS)	80	0.28
Cross-section data set	NDP	$\chi^2$
CERN-NMC [62] (DIS)	292	1.38
CERN-BCDMS [63] (DIS)	351	1.15
DESY-HERMES [67] (DIS)	81	0.45

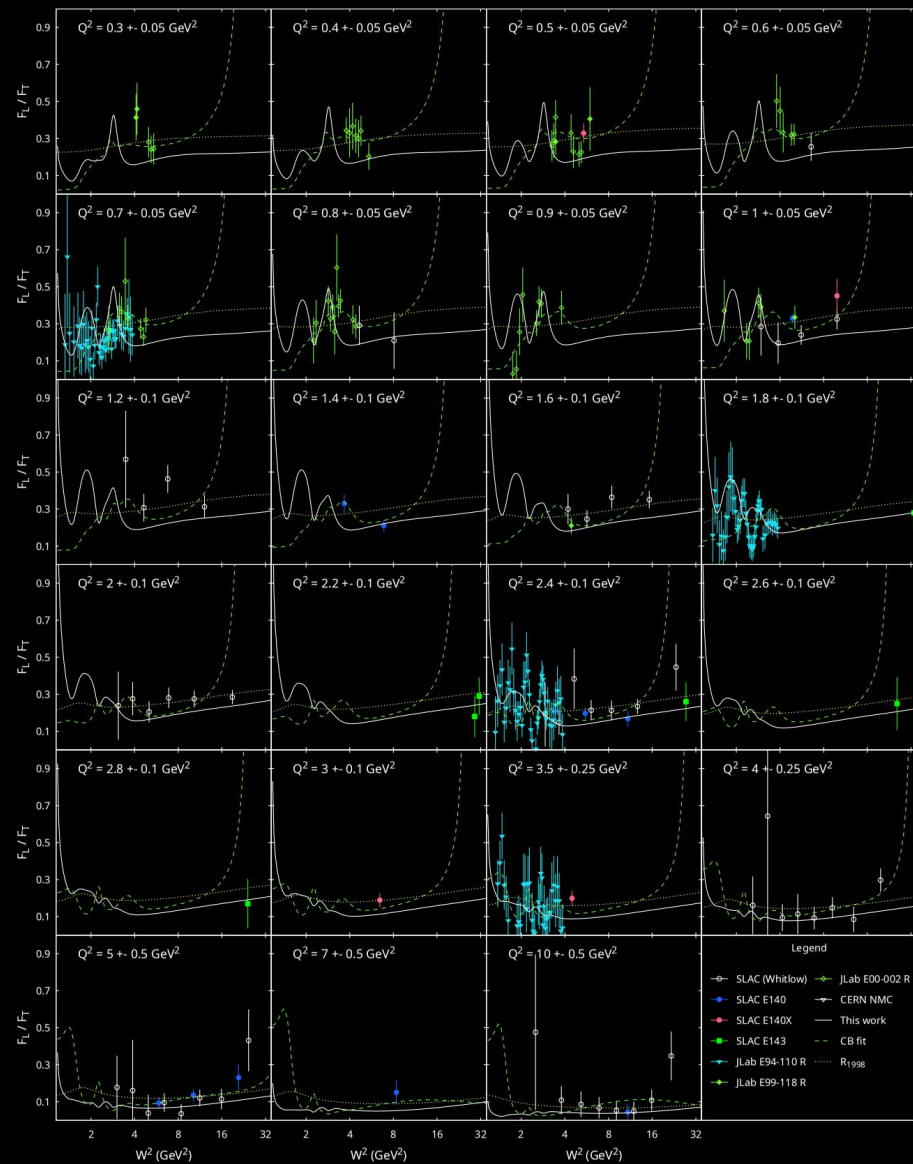
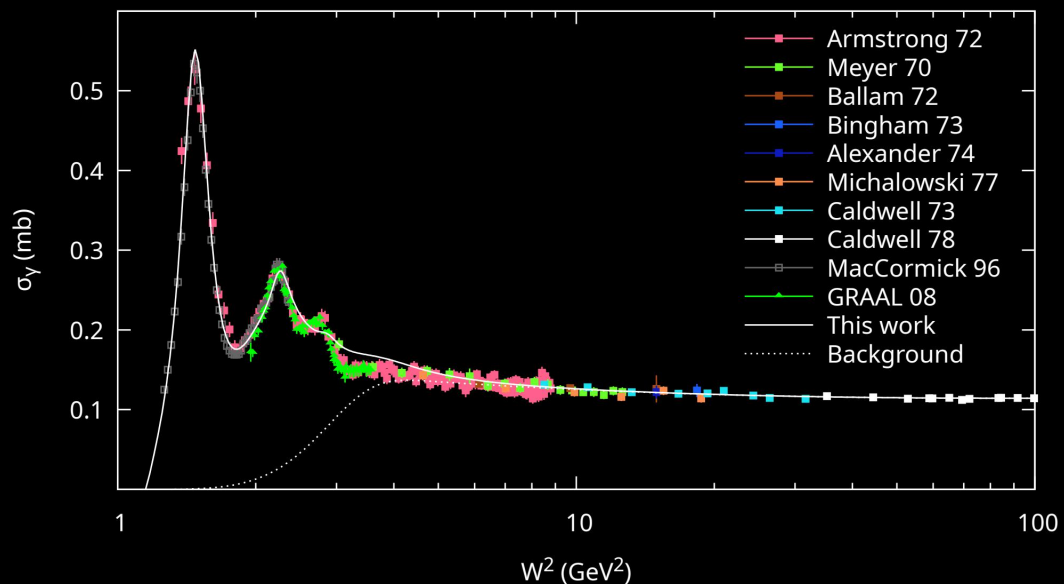
## Resonance ( $W^2 < 4 \text{ GeV}^2$ )



## DIS ( $W^2 > 4 \text{ GeV}^2$ )

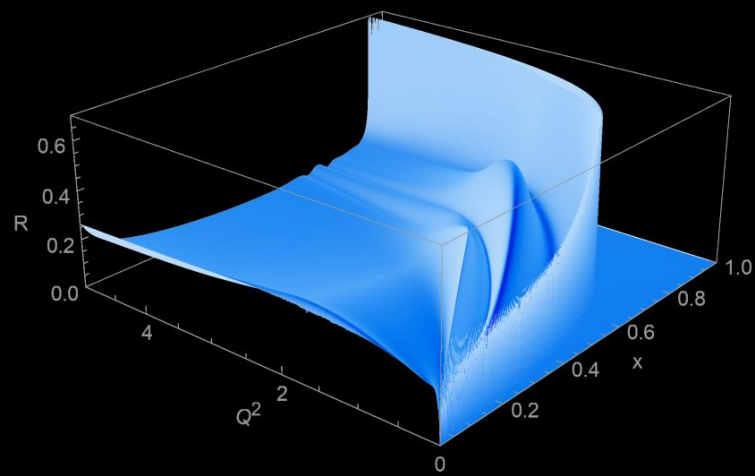
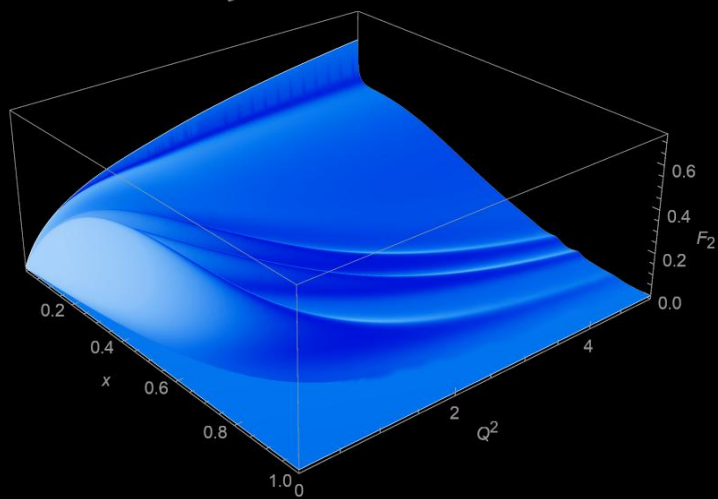
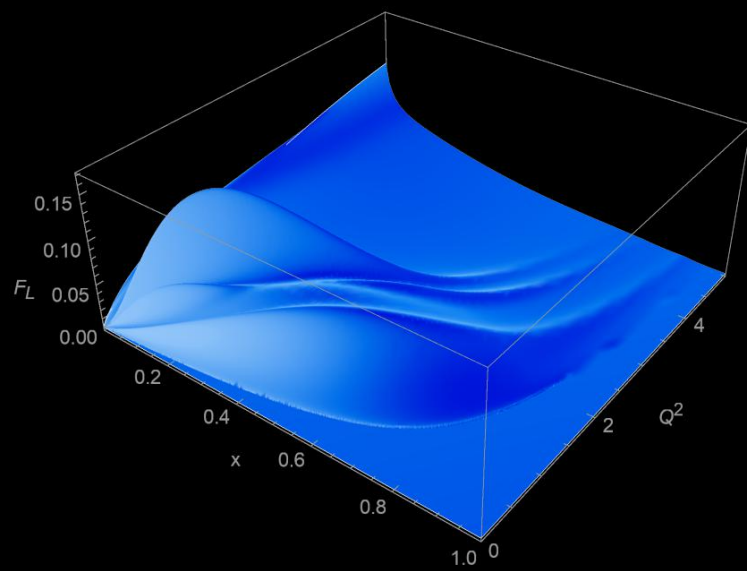
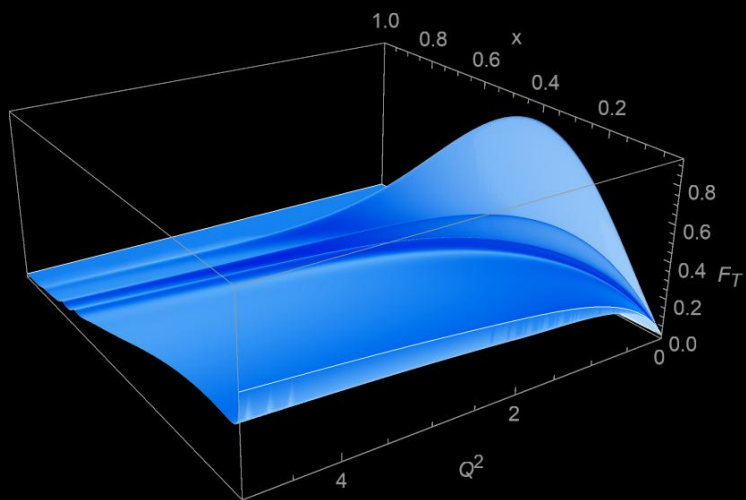


# Photoproduction and R Data Results





# Visualization



# Conclusions and Outlook

- We developed a hybrid model of the proton structure functions applicable in a wide region of  $Q^2$  and  $W^2$ .
- In the nucleon resonance region,  $W < 2$  GeV, we account for contributions from the  $\Delta(1232)$  resonance, the  $N(1440)$  Roper resonance, and three more heavy effective resonances responsible for the second and third resonance regions in the spectra.
- Nonresonant background is computed in terms of DIS structure functions properly continued into a low- $Q$  and low- $W$  region. Our extrapolation method respects the pion production threshold as well as the  $Q^2 \rightarrow 0$  real photon limit. The onset of a low- $Q$  region is defined by the parameter  $Q_0$ , the scale from which we start extrapolations of DIS SFs. The value  $Q_0^2 = 2$  GeV<sup>2</sup> provides an optimum description of electroproduction data in our analysis. The DIS region of  $Q > Q_0$  and  $W > 2$  GeV is well described in terms of the proton PDFs and the higher-twist terms from a global QCD analysis.
- The model parameters, such as resonance masses and widths, parameters of resonance helicity amplitudes, scale parameter for transition region, as well as parameters responsible for extrapolation to low- $Q$  and low- $W$  values, are adjusted from a global fit to the world data on hydrogen electroproduction and photoproduction cross section. This approach allows us to determine parameters of both the transverse and the longitudinal SFs reproducing available cross-section data with a very good accuracy.
- we verified that our hybrid model of structure functions is dual in the integral sense to the underlying DIS structure functions. The duality relation holds with a good accuracy for  $F_2$ .
- Work is in progress on extending this approach to determine parameters of the neutron structure functions from a combined set of the proton and nuclear data. Also in progress is the generalization of this model to neutrionucleon scattering in the resonance and DIS transition region, which is of primary importance for interpretation of data from current and future neutrino experiments.

# ACKNOWLEDGMENTS

*We thank S. Alekhin, A. Kataev, and R. Petti, for useful discussions, and M. Osipenko for providing the data of the JLab-CLAS Collaboration. V.V.B. was supported by the BASIS Foundation for the Development of Theoretical Physics and Mathematics*

*Thank you for your attention!*